The salivary, metal-binding peptide histatin-5 buffers extracellular copper availability

Louisa Stewart[1$], YoungJin Hong[1$], Isabel Holmes[1], Samantha Firth[1], Jack Bolton[1], Yazmin Santos[2], Steven Cobb[2], Nicholas Jakubovics[3], Karrera Djoko[1]*

[$]These authors contributed equally to the experimental work. LS is listed first to acknowledge greater involvement in manuscript preparation and editing.

[1]Department of Biosciences, Durham University, Durham DH1 3LE, United Kingdom
[2]Department of Chemistry, Durham University, Durham DH1 3LE, United Kingdom
[3]School of Dental Sciences, Newcastle University, Newcastle, United Kingdom.

*Corresponding author
karrera.djoko@durham.ac.uk

Keywords: antimicrobial peptide, histatin, copper, nutritional immunity, Streptococcus

ABSTRACT

The family of human salivary histidine-rich peptides known as histatins bind zinc (Zn) and copper (Cu), but whether they contribute to nutritional immunity by influencing Zn and/or Cu availability has not been examined. Here we tested whether histatin-5 (Hst5) limits Zn availability (and promotes bacterial Zn starvation) and/or raises Cu availability (and promotes bacterial Cu poisoning). Group A *Streptococcus* (GAS), which colonises the human oropharynx, was used as a model bacterium. Contrary to our hypothesis, Hst5 did not strongly influence Zn availability. This peptide did not induce expression of Zn uptake genes in GAS, nor did it suppress growth of an Δ*adcAI* mutant strain that is impaired in Zn uptake. Equilibrium competition measurements confirmed that Hst5 binds Zn weakly and does not compete with the high-affinity Zn uptake protein AdcAI for binding Zn. By contrast, Hst5 bound Cu with a high affinity and strongly influenced Cu availability. However, contrary to our hypothesis, Hst5 did not promote Cu toxicity. Instead, this peptide suppressed expression of Cu-inducible genes in GAS, stopped intracellular accumulation of Cu, and rescued growth of a Δ*copA* mutant strain that is impaired in Cu efflux in the presence of added Cu. These findings led us to propose a new role for Hst5 and salivary histatins as major Cu buffers in saliva that reduce the potential negative effects of Cu exposure to microbes. We speculate that histatins promote oral and oropharyngeal health by contributing to microbial homeostasis in these host niches.

IMPORTANCE

Saliva influences colonisation of the human oral cavity and oropharynx by commensal microbes, and infection (and subsequent transmission) by pathogenic microbes. This fluid assists with microbial attachment to host tissues, supplies nutrients, and buffers pH. It is thus not surprising that reduced saliva flow is a risk factor for oral and oropharyngeal dysbiosis, linked to the disappearance of beneficial microbes, overgrowth of opportunistic pathogens, and loss of microbial diversity. Our work suggests an additional role for saliva, particularly the salivary metal-binding peptides histatins, in buffering the availability of metal ions such as copper. In doing so, histatins may contribute to microbial homeostasis by safeguarding resident microbes from potential copper toxicity, which can arise from endogenous (metal-linked immune response to pathogens) or exogenous (food, medicine) sources. Our study raises exciting questions about potential functions of host metal-binding peptides in controlling metal availability in ways that support (instead of suppress) host-associated microbes.

INTRODUCTION

Metals are essential micronutrients. Like all nutrients, too little of any metal will cause starvation, but too much will cause toxicity. Metal levels and those of metal-binding proteins within a multicellular host organism can rise and fall in response to microbial infection, leading to fluctuations in metal availability within different niches in the infected host. Where metal availability decreases, invading microbes encounter metal starvation and accordingly upregulate metal uptake. Where it increases, microbes encounter toxicity and, in response, upregulate metal efflux and sequestration. These antagonistic host responses are known as “nutritional immunity”[1] and are key components of host-pathogen interactions.

Antimicrobial peptides (AMPs) are short peptides that are secreted by diverse host organisms[2]. These peptides act usually as immune effectors that kill microbes as part of the host innate immune defence, but many also play key functions in the normal biology of the host organism. Several AMPs bind metals. Some become activated upon metal binding, for instance by folding into an optimal conformation for acting on their targets (*e.g.* piscidin from fish[3]). Others bind metals and potentially withhold these essential nutrients from microbes (*e.g.* microplusin from cattle ticks[4, 5]).

Human salivary histatins comprise a family of cationic, His-rich AMPs that are all derived from two parent peptides, namely Histatin-1 and Histatin-3[6, 7]. Both histatins are expressed constitutively and exclusively by the salivary glands of humans and some higher primates[7, 8]. Upon secretion into the oral cavity, histatins are rapidly processed into shorter fragments[9, 10] by unidentified human salivary proteases or proteases from resident oral microbes. Of these fragments, Histatin-5 (Hst5; Table 1) is the best characterised.

Table 1. Hst5 peptides and variants used in this work.

Peptide	Sequence
Hst5	DSHAKRHHGY KRKFHEKHHS HRGY
ΔH3	ASAAKRHHGY KRKFHEKHHS HRGY
ΔH3,7	DSAAKRAHGY KRKFHEKHHS HRGY
ΔH7,8	DSHAKRAAGY KRKFHEKHHS HRGY
ΔH15,18,19	DSHAKRHHGY KRKFAEKAAS HRGY

Hst5 is noted for its direct antimicrobial activity, especially against the fungus *Candida albicans*[11, 12]. Unlike other AMPs, Hst5 does not permeabilise fungal membranes, although it does destabilise some bacterial membranes[12]. Beyond its direct action on membranes, the antimicrobial activity of Hst5 requires the peptide to be internalised into the cytoplasm[12, 13], usually *via* energy-dependent pathways for peptide uptake. Once in the cytoplasm, Hst5 encounters its targets and causes toxicity *via* multiple pathways that are not fully elucidated[11, 14].

Hst5 is also noted for its metal-binding properties. Unsurprisingly, this peptide is speculated, though not demonstrated, to participate in nutritional immunity[11]. Hst5 contains the characteristic

Zn-binding motif His-Glu-x-His-His (Table 1), but whether Zn binding is essential for the antimicrobial activity of this peptide is unclear. Hst5 derivatives that lack one or all three His residues remain active against *C. albicans*[15], and conflicting reports show that addition of Zn can both enhance[16] and suppress[17] Hst5 activity against this fungus. Hst5 also possesses three Cu-binding motifs, namely the N-terminal ATCUN motif that binds Cu(II) and two *bis*-His motifs that bind one Cu(I) each (Table 1)[18]. Addition of Cu potentiates the activity of Hst5 against *C. albicans*[18]. This potentiation relies on the Cu(I) site but not the Cu(II) site[18].

This study explored the relationship between Hst5 and metals, particularly Zn and Cu, and examined the potential role of Hst5 in influencing metal availability during nutritional immunity. Based on the reported metal-dependent effects of Hst5 against *C. albicans* and on established features of nutritional immunity, we hypothesised that Hst5 either limits Zn availability (and promotes microbial Zn starvation) and/or raises Cu availability (and promotes Cu poisoning). To test this hypothesis, the Gram-positive human pathogen *Streptococcus pyogenes* (Group A *Streptococcus*, GAS) was used as a model. This pathogen colonises the human throat, where it comes into contact with saliva and salivary components, but its interactions with Hst5 have not been described previously. Secondly, pathways for metal homeostasis in GAS are relatively well understood and phenotypes of mutant strains lacking key metal transport proteins are known[19]. These features enabled GAS to be exploited here as a tractable, well-defined experimental tool for examining the metal-dependent effects of Hst5.

RESULTS

Hst5 does not exert direct antibacterial effects against GAS.

The effects of Hst5 on growth of GAS were examined in a metal-deplete, chemically defined medium (CDM-glucose)[20]. In this medium, up to 50 µM Hst5 (*ca.* total histatin concentrations in fresh salivary secretions[10]) did not affect growth of wild-type GAS (Figure 1A). Identical results were obtained in THY medium (Figure S1A).

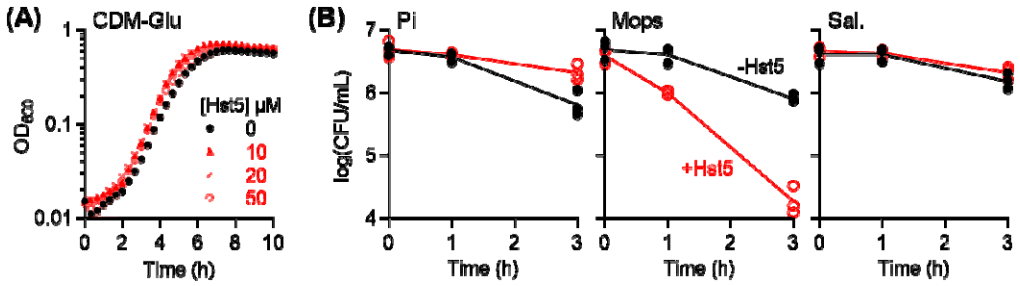

Figure 1. Effects of Hst5 on (A) growth and (B) survival of GAS. (A) Bacteria were cultured in CDM-glucose (n = 2) in the presence of Hst5 (0, 10, 20, 50 µM). **(B)** Bacteria (n = 3) were incubated in dilute phosphate buffer (10 mM, pH 7.4; Pi), Na-Mops buffer (10 mM, pH 7.4; Mops), or artificial saliva salts (pH 7.2-7.4, *cf.* Dataset S1a; Sal.), with (empty circles) or without (filled circles) Hst5 (50 µM).

The effects of Hst5 on GAS viability were examined in 10 mM phosphate buffer, following procedures described previously for *C. albicans* and ESKAPE pathogens[12, 16]. Under these conditions, up to 50 µM Hst5 did not kill GAS (Figure 1B). Instead, Hst5 prolonged survival of this bacterium (Figure 1B). A parallel control experiment showed that, as reported elsewhere[12], the same concentrations of Hst5 killed *Pseudomonas aeruginosa* within minutes (Figure S2A), confirming that our peptide stocks were active.

Like other cationic AMPs, the antimicrobial activity of Hst5 relies on initial electrostatic binding of the peptide to microbial surface proteins or membranes[12, 21]. Such interactions are suppressed by salts and high ionic strength buffers[12, 15, 22-26]. To lower the ionic strength in our experiments, phosphate was replaced with Mops. Under these new conditions, Hst5 *did* kill GAS (Figure 1B). However, carryover salts from solutions used in preparing the inoculum abolished this killing effect (Figure S2B), underscoring the sensitivity of these assays to salt.

To better reflect the physiological conditions in which Hst5 is found, we repeated the killing assay in buffered “artificial saliva salts”, whose salt composition approximates healthy saliva (Dataset S1a). Hst5 did *not* kill GAS under these conditions (Figure 1B), confirming that the results in phosphate buffer are more physiologically relevant. For ease of comparison with existing literature, further experiments described below used phosphate buffer.

The lack of a direct antibacterial effect against GAS adds to the list of contradictory effects of Hst5 against streptococci reported in the literature[27-32]. Given the sensitivity of these assays to ionic strength[15, 22-26] and peptide purity or identity[9, 33], the effects of Hst5 on GAS and five oral streptococci, namely *S. anginosus*, *S. mutans*, *S. oralis*, *S. salivarius*, and *S. sanguinis*, were examined here in parallel. Hst5 did not kill or inhibit the growth of any of the streptococci under these conditions (Figure 2, Figure S1B). In fact, Hst5 promoted growth of *S. anginosus*, *S. oralis*, and, to a lesser extent, *S. sanguinis*. The mechanism behind this growth-promoting activity of Hst5 is beyond the scope of the present work, but is potentially related to the metal-chelating ability of this peptide (described below). Nonetheless, it can be concluded that Hst5 does not exert a direct anti-streptococcal activity.

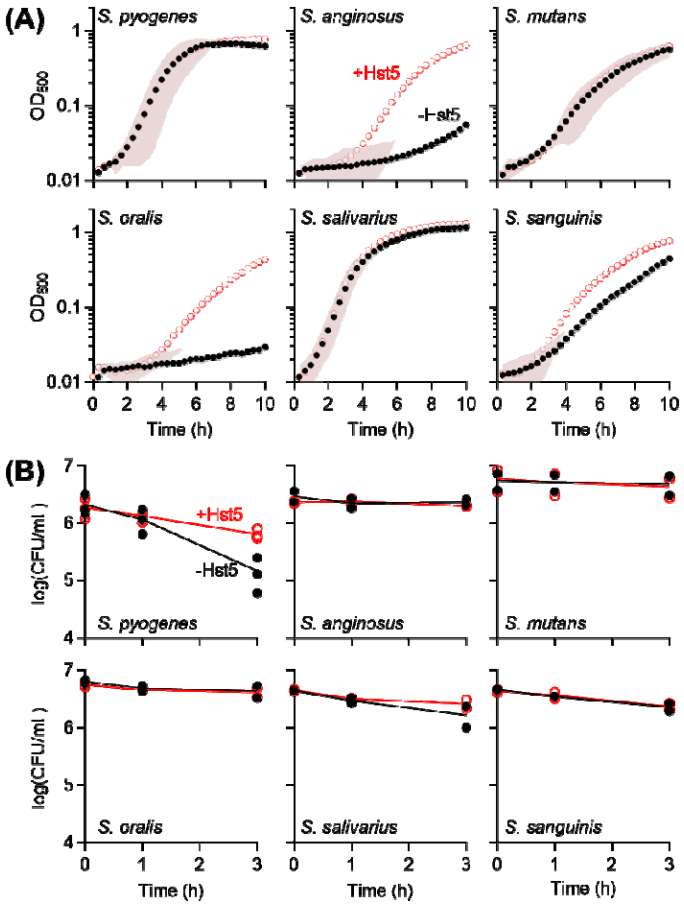

Figure 2. Effects of Hst5 on (A) growth and (B) survival of oral streptococci. (A) Bacteria were cultured in CDM-glucose (*n* = 2) with (empty circles) or without (filled circles) Hst5 (50 µM). **(B)** Bacteria (*n* = 2) were incubated in dilute phosphate buffer (10 mM, pH 7.4) with (empty circles) or without (filled circles) Hst5 (50 µM).

Hst5 does not strongly influence Zn availability.

To contribute to nutritional immunity, Hst5 may: (i) bind and sequester Zn, limit Zn availability to GAS, and cause Zn starvation (Figure 3); or (ii) increase Zn availability, promote influx or accumulation of Zn in GAS, and cause Zn poisoning. However, adding up to 50 µM Zn (equimolar with Hst5 and in excess of Zn concentrations in whole saliva[34]) neither suppressed nor enhanced the direct effects of Hst5 on GAS (Figure 4, Figure S1C).

Zn starvation or poisoning may not cause a direct killing or inhibitory effect against wild-type GAS, since the transcriptionally-responsive system for Zn homeostasis responds to, and thus counters, perturbations in Zn availability. This system (Figure 3) consists of the co-repressor AdcR[35], which upregulates expression of Zn uptake genes (*e.g. adcAI*, *adcAII*) in response to Zn limitation, and the de-repressor GczA[36], which induces expression of a Zn efflux gene (*czcD*) in response to Zn excess.

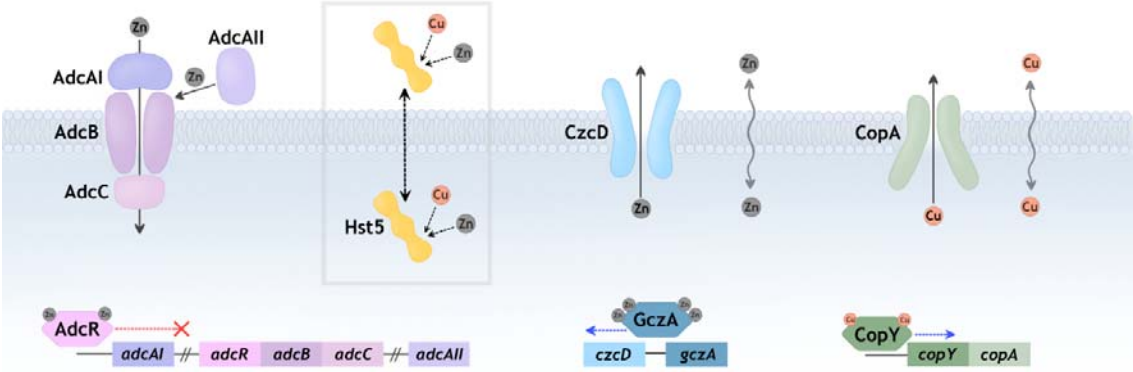

Figure 3. Metal homeostasis in GAS and hypothesised actions of Hst5. Zn uptake: AdcAI and AdcAII capture Zn from the extracellular environment and transfer this metal to AdcBC for import into the cytoplasm. Expression of these proteins is transcriptionally upregulated by AdcR in response to decreases in Zn availability and repressed in response to increases in Zn availability. **Zn efflux:** CzcD exports excess Zn out of the cytoplasm. Its expression is transcriptionally upregulated by GczA in response to increases in Zn availability and repressed in response to decreases in Zn availability. **Cu efflux:** CopA exports excess Cu out of the cytoplasm. Its expression is transcriptionally upregulated by CopY in response to increases in Cu availability. **Hypothesised actions of Hst5:** Hst5 may remain extracellular, bind Zn or Cu, and suppress extracellular metal availability. Alternatively, Hst5 may become internalised, bind Zn or Cu in the cytoplasm, and suppress intracellular metal availability. Hst5 may also become internalised as the Zn-Hst5 or Cu-Hst5 complex, facilitate entry of Zn or Cu into the cytoplasm, and increase metal availability.

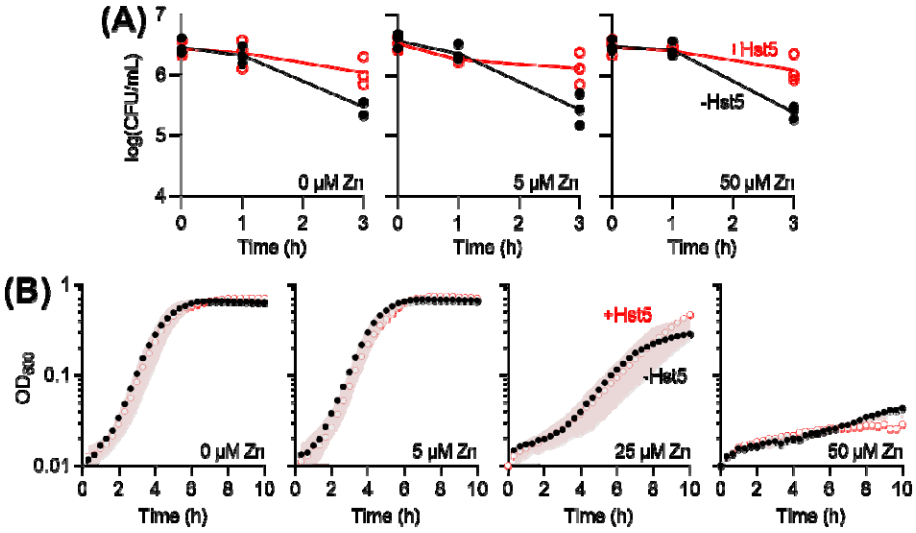

Figure 4. Effects of Zn on (A) survival and (B) growth of GAS in the presence of Hst5. (A) Bacteria (*n* = 3) were incubated in phosphate buffer in the presence of Zn (0, 5, 50 µM) with (empty circles) or without (filled circles) Hst5 (50 µM). **(B)** Bacteria (*n* = 3) were cultured in CDM-glucose in the presence of Zn (0, 5, 25, 50 µM) with (empty circles) or without (filled circles) Hst5 (50 µM).

Expression of the three Zn-responsive genes listed above (*adcAI*, *adcAII*, *czcD*) was examined accordingly. Only bacteria grown in CDM-glucose were used for analyses, since poor RNA yields were obtained from bacteria that were incubated in phosphate buffer, likely associated with the progressive loss of viability under these conditions (*cf.* Figure 1B). In our control experiment, adding Zn alone did not further repress transcription of *adcAI* and *adcAII*, but it did induce expression of *czcD* (Figure S3A), consistent with an increase in Zn availability. Conversely, adding the Zn chelator TPEN did not affect transcription of *czcD*, but it did induce expression of both *adcAI* and *adcAII*, consistent with a decrease in Zn availability (Figure S3B). By contrast, adding Hst5 alone perturbed neither the basal expression of *adcAI* or *adcAII* (Figure 5A), nor the Zn-dependent expression of *czcD* (Figure 5B). These results indicate that Hst5 neither induces Zn limitation nor promotes Zn poisoning in GAS, respectively.

As described earlier, Zn uptake by AdcAI and Zn efflux by CzcD may mask the effects of Hst5 on Zn availability (Figure 3). To unmask these effects, the antibacterial activity of Hst5 was re-examined using the Δ*adcAI* and Δ*czcD* mutant strains. The control experiment confirmed that these mutant strains were sensitive to growth inhibition by TPEN[37, 38] and added Zn[36, 38], respectively (Figure S4). Although additional Zn-binding lipoproteins such as AdcAII contribute to Zn acquisition[37], AdcAI is thought to act as the primary Zn importer[37, 38]. Therefore, only the Δ*adcAI* mutant was employed here for investigation.

Hst5 exerted similar antibacterial effects on the wild type and Δ*adcAI* mutant strains. Treatment with Hst5 did not perturb growth of the Δ*adcAI* mutant strain in CDM-glucose (Figure 5C, *cf.* Figure 1A for the wild type). When examined in phosphate buffer, treatment with Hst5 improved (instead of reduced) survival of the Δ*adcAI* mutant strain (Figure 5D). These observations strengthen the proposal that Hst5 does not starve GAS of nutrient Zn.

The effects of Hst5 treatment on survival of the Δ*czcD* mutant in phosphate buffer were also comparable to those on the wild type. Adding up to 50 µM Zn did not impact survival of either strain (Figure 5E). Therefore, Zn does not exert significant toxicity under these conditions and Hst5 does not potentiate it. When examined in CDM-glucose, Hst5 weakly rescued (instead of further inhibited) growth of the Δ*czcD* mutant in the presence of added Zn (Figure 5F). This growth-promoting effect became apparent upon comparing final culture densities (Figure 5G), since exponential growth rates remained unchanged (Figure 5H). It was observed only over a narrow range of added Zn concentrations (between 5–10 µM Zn; Figure 5G). This growth-promoting effect of Hst5 appeared to require the predicted Zn-binding ligands His15, His18, and His19[39, 40], since growth of the Zn-treated Δ*czcD* mutant in the presence of the ΔH15,18,19 variant of Hst5 was indistinguishable with growth in the absence of Hst5 (Figure S5A-B). The roles of the other His residues were less clear (Figure S5A-B). Nevertheless, it can be concluded that Hst5 does not potentiate Zn toxicity to GAS.

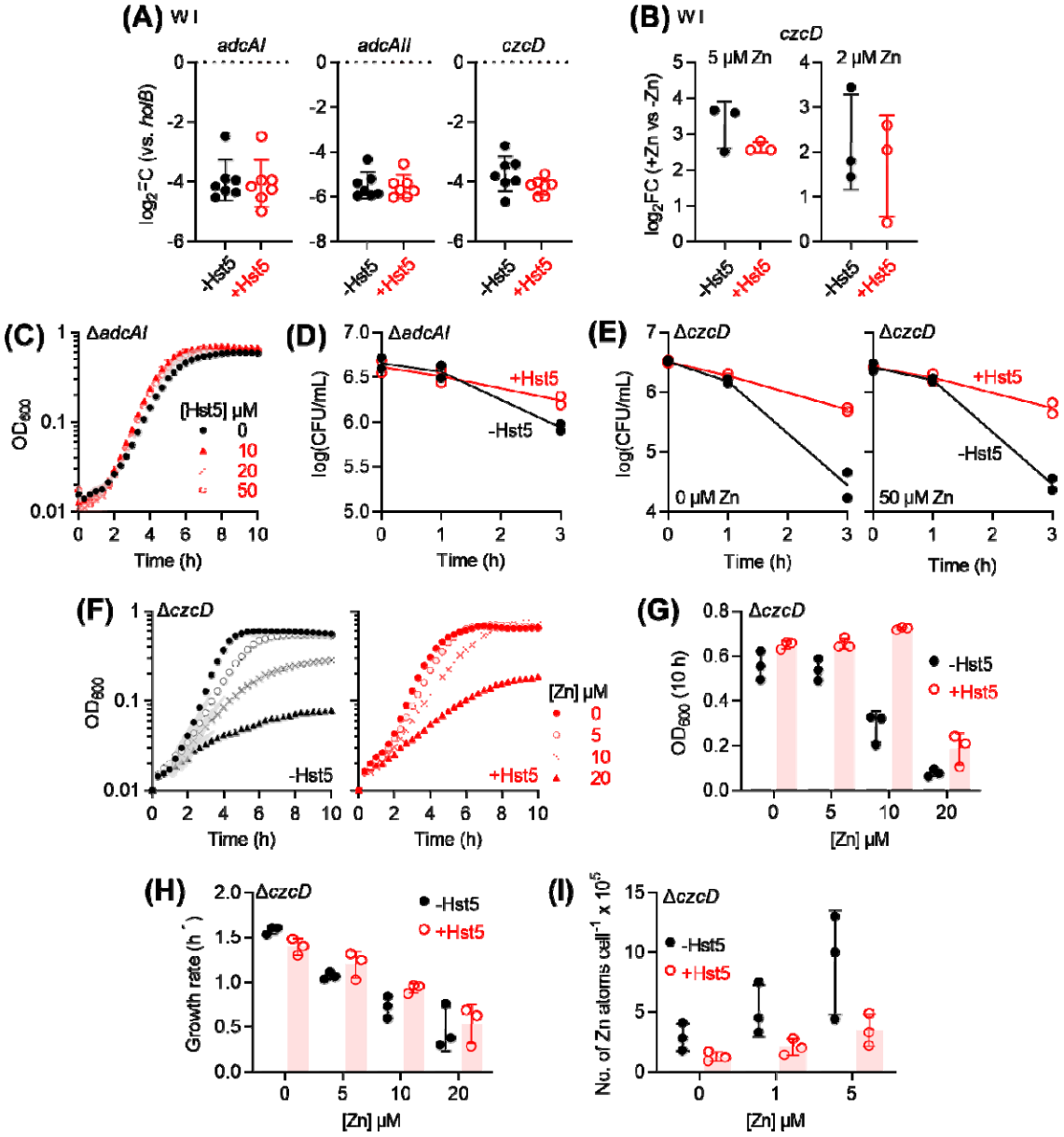

Figure 5. Effects of Hst5 on Zn availability. (A) Expression of Zn homeostasis genes. Bacteria (*n* = 7) were cultured in CDM-glucose with (empty circles) or without (filled circles) Hst5 (50 µM). Levels of *adcAI*, *adcAII*, and *czcD* mRNA were determined by qRT-PCR and normalised to *holB*. **(B) Zn-dependent expression of *czcD*.** Bacteria (*n* = 3) were cultured in CDM-glucose in the presence of added Zn (2 or 5 µM), with (empty circles) or without (filled circles) Hst5 (50 µM). Levels of *czcD* mRNA were measured by qRT-PCR, normalised to *holB*, and compared to normalised mRNA levels of the corresponding untreated controls (0 µM added Zn). **(C) Growth of Δ*adcAI*.** Bacteria (*n* = 2) were cultured in CDM-glucose with or without Hst5 (0, 10, 20, 50 µM). **(D) Survival of Δ*adcAI*.** Bacteria (*n* = 2) were incubated in dilute phosphate buffer with (empty circles) or without (filled circles) Hst5 (50 µM). **(E) Survival of Δ*czcD*.** Bacteria (*n* = 2) were incubated in dilute phosphate buffer in the presence or absence of Zn (50 µM) with (empty circles) or without (filled circles) Hst5 (50 µM). **(F) Growth of Δ*czcD*.** Bacteria (*n* = 3) were cultured in CDM-glucose in the presence of Zn (0 – 20 µM)

with (empty circles) or without (filled circles) Hst5 (50 µM). **(G) Final culture densities from panel F. (H) Growth rates from panel F. (I) Intracellular Zn levels in Δ*czcD*.** Bacteria (*n* = 3) were cultured in CDM-glucose with or without Hst5 (50 µM), in the presence of Zn (0, 1, or 5 µM). Intracellular levels of Zn were measured by ICP MS and normalised to colony counts.

Two mechanistic models are compatible with the protective effects of Hst5 under conditions of Zn stress (*cf.* Figure 3): (i) Hst5 acts as an extracellular Zn buffer that weakly suppresses entry of this metal ion into the GAS cytoplasm, leading to less Zn toxicity, or (ii) Hst5 acts as an intracellular Zn buffer that enables more Zn to accumulate in the cytoplasm, but with less toxicity. Hst5 treatment would decrease intracellular Zn levels in the first model but increase in the second.

To test the above proposals, total intracellular Zn levels in the Δ*czcD* mutant strain were assessed by ICP MS. Only up to 5 µM Zn was used, since adding 10 µM Zn inhibited growth of this mutant strongly and did not produce sufficient biomass for metal analyses. Only the wild-type peptide was used in these experiments, owing to the large culture volumes required for metal analyses and the high cost of peptide synthesis.

Figure 5I shows that growth in the presence of added Zn increased intracellular Zn levels in the Δ*czcD* mutant, but co-treatment with Hst5 suppressed this effect. These results initially appeared to support the first model, in which Hst5 acts as an extracellular Zn buffer. However, we noted that intracellular Cu levels in these samples were similarly elevated in the absence of Hst5 and similarly suppressed in the presence of Hst5 (Figure S5C). At this stage, we cannot exclude the possibility that Zn treatment led to spurious effects associated with the observed growth defect. Thus, while our data hint at a role for Hst5 as a weak extracellular Zn buffer that weakly influences excess Zn availability to GAS, they are not conclusive, particularly when compared with the clear role of Hst5 as a strong Cu buffer (see below).

Hst5 acts as an extracellular Cu(II) buffer that strongly limits Cu availability.

Based on the reported synergy between Hst5 and Cu against *C. albicans*, we hypothesised that Hst5 promotes Cu toxicity to GAS. However, adding up to 50 µM of Cu (equimolar with Hst5; *ca.* 10X higher than Cu concentrations in saliva[41-43]) neither enhanced nor suppressed the effect of Hst5 against wild-type GAS (Figure 6; *cf.* Figure S1D for results in THY).

As in the case with Zn, any effect of Hst5 on Cu availability may not lead to a direct killing or inhibitory effect against wild-type GAS. This bacterium possesses the CopYAZ system for exporting Cu, which is transcriptionally upregulated by the de-repressor CopY in response to added Cu[44] (Figure 3). The transcriptional response of this CopY system was examined here to probe the Cu-linked action of Hst5.

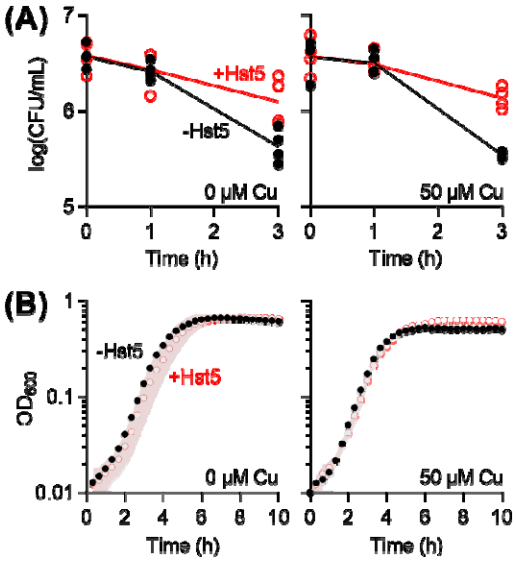

Figure 6. Effects of Cu on (A) survival and (B) growth of GAS in the presence of Hst5. **(A)** Bacteria (*n* = 5) were incubated in dilute phosphate buffer in the presence of added Cu (0 or 50 µM) with (empty circles) or without (filled circles) Hst5 (50 µM). **(B)** Bacteria (*n* = 3) were cultured in CDM-glucose in the presence of added Cu (0 or 50 µM) with (empty circles) or without (filled circles) Hst5 (50 µM).

Our control experiment confirmed that GAS grown in CDM-glucose was Cu-deplete, since adding the extracellular Cu chelator BCS did not further repress expression of the CopY-regulated genes *copA* and *copZ* (Figure S3C). Conversely, adding Cu induced expression of both genes (Figures S3D, Figure 7A), consistent with an increase in Cu availability[20]. Co-treatment with Hst5 suppressed this Cu-dependent induction (Figure 7A). This effect required the predicted Cu(II) binding site[18, 45], since the ΔH3 and ΔH3,7 variants lacking His3 were less effective at reducing expression *copA* and *copZ* (Figure 7B). By contrast, it did not require the predicted Cu(I) binding sites[18], since the effects of the ΔH7,8 and ΔH15,18,19 variants lacking either of the *bis*-His motifs were indistinguishable to that of the wild-type peptide (Figure 7B). Together, these observations led us to propose that Hst5 acts as a Cu(II)-specific buffer that suppresses accumulation of Cu in the GAS cytoplasm.

To test the above proposal, we employed the Cu-sensitive Δ*copA* mutant that lacks the Cu-effluxing P-type ATPase (Figure 3). Survival assays in phosphate buffer revealed no difference between survival of this mutant strain and that of the wild type (Figure 7C). Therefore, Cu did not exert significant toxicity under these conditions and Hst5 did not amplify it. When examined in CDM-glucose, adding Cu suppressed growth of the Δ*copA* mutant in the late exponential phase of growth (Figure 7D), as reported previously[20]. Co-treatment with Hst5 rescued growth of this mutant completely (Figure 7D). Again, this protective effect required the His3 ligand for Cu(II), but neither of the two *bis*-His ligands for Cu(I) (Figure 7E, Figure S6A). These results further support our hypothesis that Hst5 acts as a Cu(II)-specific buffer.

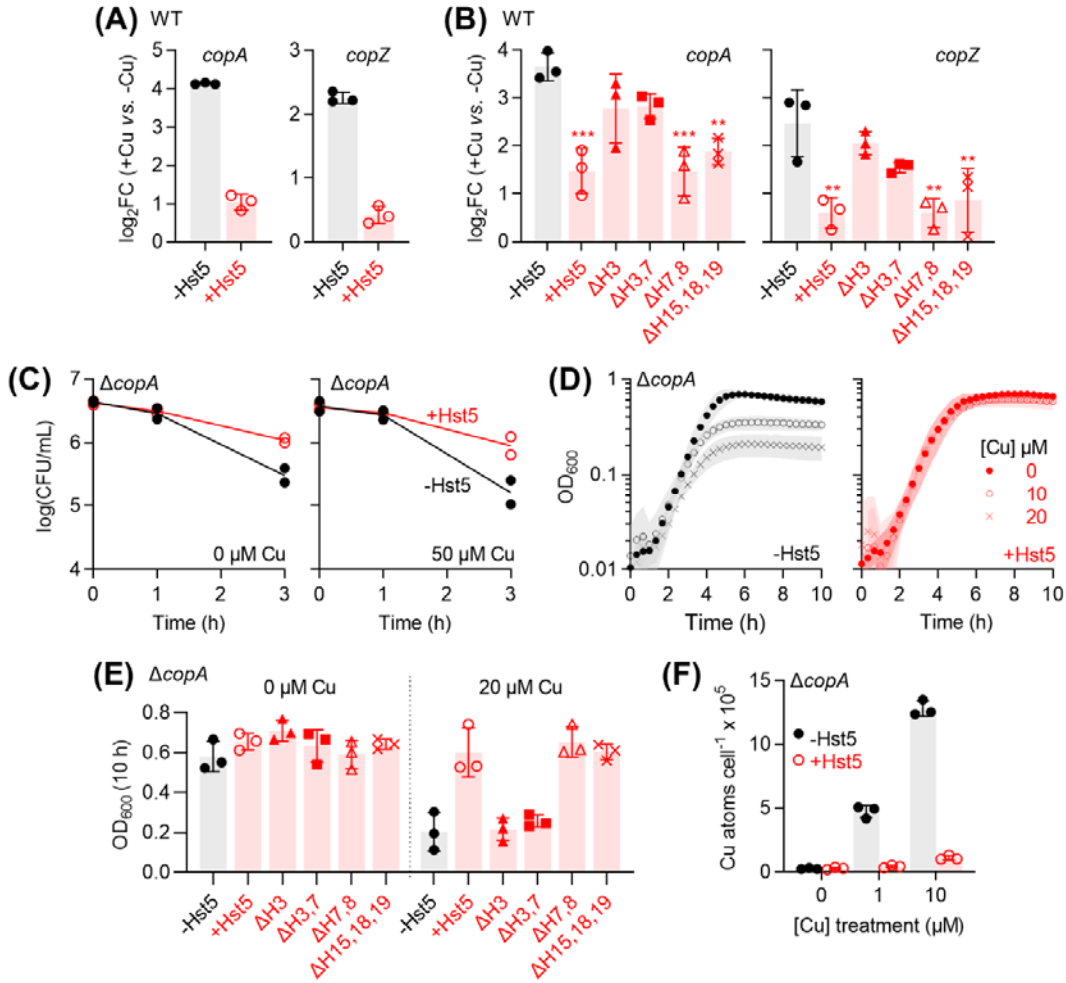

Figure 7. Effects of Hst5 on Cu availability. (A) Expression of Cu homeostasis genes. Bacteria (*n* = 3) were cultured in CDM-glucose in the presence of added Cu (10 μM Cu), with or without Hst5 (50 μM). Levels of *copA* and *copZ* mRNA were measured by qRT-PCR, normalised to *holB*, and compared with normalised mRNA levels of the corresponding untreated controls (0 μM Cu). **(B) Effects of Hs5 variants on expression of Cu homeostasis genes.** The experiment was performed as described in panel A. The following treatments suppressed Cu-dependent *copA* expression when compared with untreated control: Hst5 (***P = 0.0003), ΔH7,8 (***P = 0.0003), ΔH15,18,19 (**P = 0.0018). The following treatments had no effect: ΔH3 (P = 0.1), ΔH3,7 (P = 0.2). The following treatments suppressed Cu-dependent *copZ* expression when compared with untreated control: Hst5 (***P = 0.001), ΔH7,8 (***P = 0.001), ΔH15,18,19 (**P = 0.003). The following treatments had no effect: ΔH3 (P = 0.7), ΔH3,7 (P = 0.1). **(C) Survival of Δ*copA*.** Bacteria (*n* = 2) were incubated in dilute phosphate buffer in the presence or absence of Cu (50 μM) with (empty circles) or without (filled circles) Hst5 (50 μM). **(D) Growth of Δ*copA*.** Bacteria (*n* = 3) were cultured in CDM-glucose with or without Hst5 (50 μM), in the presence of added Cu (0 – 20 μM). **(E) Effects of Hst5 variants on growth of Δ*copA*.** Bacteria (*n* = 3) were cultured in CDM-glucose in the presence of added Cu (0 or 20 μM) with or without Hst5 or its variants (50 μM). Complete growth curves are shown in Figure S6. For ease of comparison, only OD_{600} values from the end of the experiment (t = 10 h) were plotted

here. **(F) Intracellular Cu levels in Δ*copA*.** Bacteria (*n* = 3) were cultured in CDM-glucose in the presence of Cu (0, 1 or 10 µM) with or without Hst5 (50 µM). Intracellular levels of Cu were measured by ICP MS and normalised to colony counts.

Two models are again plausible (*cf.* Figure 3): (i) Hst5 buffers extracellular Cu and suppresses entry of Cu into the GAS cytoplasm, leading to less Cu toxicity, or (ii) Hst5 buffers intracellular Cu, allowing intracellular Cu levels to rise without significant toxicity. The latter would resemble the model described recently for GSH in buffering excess intracellular Cu[20]. Since Cu(II) is not thought to exist within the reducing cytoplasm, the first model is more likely. Consistent with this proposal, ICP MS analyses of total metal levels in the Δ*copA* mutant confirmed that growth in the presence of Cu led to an increase in total intracellular Cu levels, but co-treatment with Hst5 strongly suppressed these levels (Figure 7F). Unlike the situation described earlier for the Δ*czcD* mutant, there were no unanticipated effects on other metal levels such as Zn (Figure S6B). Thus, it can be concluded that Hst5 acts as an extracellular Cu(II) buffer that limits Cu availability to GAS.

Molecular basis for the action of Hst5 in weakly influencing Zn availability.

Hst5 is thought to bind up to three Zn atoms. ITC measurements yielded log K_{Zn} values of 4.0, 5.0, and 5.1[45]. In agreement with Zn binding only weakly to the peptide, the Zn-Hst5 complex dissociated upon passage through a desalting column (Figure 8A).

The affinities of Hst5 to Zn were re-examined here by equilibrium competition with the colorimetric Zn indicator Zincon (log K_{Zn} ~ 6.0) and monitoring solution absorbances of *apo*-Zincon and Zn-Zincon at 466 nm and 620 nm, respectively (Figure 8B). However, the competition curve (in the presence of Hst5) was nearly indistinguishable from the control (in the absence of Hst5) (Figure 8C). In addition, a new peak at 650 nm appeared in the presence of Hst5 (Figure 8B), indicating formation of a new species, likely a ternary complex between Hst5, Zincon, and Zn. This peak did not disappear upon adding excess Hst5 (Figure 8B). These results indicate that Hst5 does not compete effectively with Zincon, and that this peptide binds Zn more weakly than previously estimated by ITC[45].

A previous study showed effective competition between Hst5 and Zincon in phosphate buffer, with Hst5 removing 2 molar equiv. of Zn from Zincon[16]. However, when used at millimolar concentrations, phosphate can become competitive for binding Zn[46]. Indeed, repeating the control titration in phosphate buffer (50 mM) instead of Mops led to clear partitioning of Zn between Zincon and the buffer (Figure S7A-B). Prolonged incubation (>10 min) of Zn-Zincon in this buffer also led to loss of the characteristic blue colour (Figure S7C). For these reasons, estimates of Zn affinity and stoichiometry of Hst5 using Zincon in Mops buffer are likely to be more reliable.

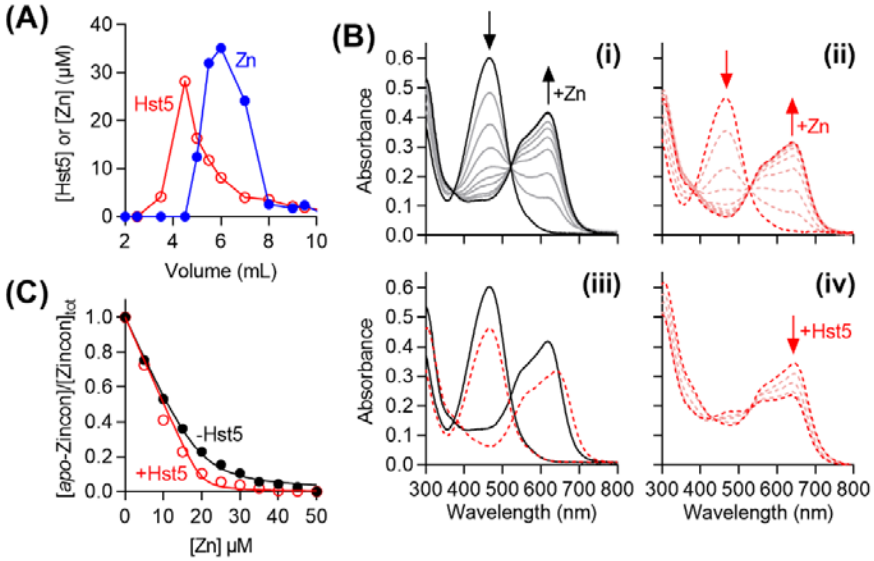

Figure 8. Zn affinity of Hst5. (A) Separation of Hst5 (empty circles) and Zn (filled circles) on a polyacrylamide desalting column. **(B)** Spectral changes upon addition of Zn (0 – 50 µM) into *apo*-Zincon (20 µM): **(i)** in the absence (solid traces) or **(ii)** presence (dashed traces) of Hst5 (20 µM). **(iii)** Overlaid spectra for 0 and 50 µM Zn from panels (i) and (ii). **(iv)** Spectral changes upon addition of excess Hst5 (0 – 200 µM) into a solution of Zn (20 µM) in *apo*-Zincon (25 µM). Upwards and downwards arrows indicate increases and decreases in absorbance intensity, respectively. **(C)** Normalised plot of the absorbance intensities of *apo*-Zincon at 467 nm upon addition of Zn in the absence (filled circles) or presence (empty circles) of Hst5 (20 µM).

The weak binding of extracellular Zn to Hst5 was clearly insufficient to starve wild-type GAS of nutrient Zn (*cf.* Figures 5A, 5C), indicating that this peptide does not compete with the high-affinity, Zn-*specific* uptake protein AdcAI (*cf.* Figure 3). AdcAI possesses two separate sites for binding Zn. ITC measurements identified one tight Zn site (log K_{Zn} = 7.0) in the N-terminal domain and one weak site (log K_{Zn} = 5.6) in the C-terminal domain[47]. Both sites appeared essential for Zn uptake[47]. Based on these affinities, Hst5 (log $K_{Zn} \leq 5.1$) may compete with the C-terminal- domain, particularly at the start of bacterial growth, when this peptide is present in excess relative to bacteria. Such a model is incompatible with our experimental data.

ITC can underestimate metal binding affinities due to lack of sensitivity, lack of specificity, and potential side reactions (*e.g.* competition with buffers)[48]. Thus, the Zn affinities of AdcAI were re-examined here by competition with the colorimetric Zn indicator Mag-fura2 (Mf2). The competition curve, generated by monitoring absorbance of *apo*-Mf2 at 377 nm, clearly showed two Zn binding sites in AdcAI (Figure 9A). One site, presumably the tight site, outcompeted Mf2, as evidenced by the lack of spectral changes upon adding up to 1 molar equiv. of Zn *vs.* AdcAI (Figure 9A). The second site, likely the weak site, competed effectively with Mf2 with a log K_{Zn} = 8.5 (±0.2), *ca.* 1000-fold tighter than previously estimated[47]. The affinity of the tight site was better estimated using Quin-2 (Q2) as the competitor. By monitoring absorbance of *apo*-Q2 at 266 nm, a log K_{Zn} = 12.5 (±0.2) was obtained for this site (Figure 9B), again *ca.* 1000-fold tighter than the previous estimate[47].

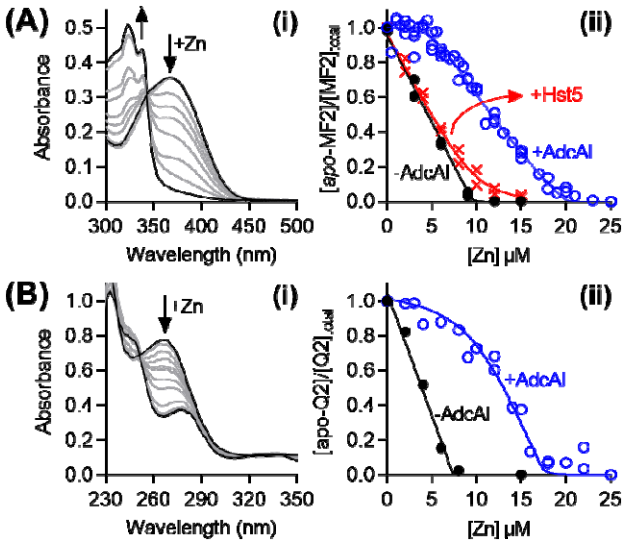

Figure 9. Zn affinity of AdcAI. (A) The weak site. (i) Spectral changes upon titration of Zn (0 – 25 µM) into a mixture of *apo*-Mf2 (10 µM) and AdcAI (5 µM). Upwards and downwards arrows indicate increases and decreases in absorbance intensity, respectively. **(ii)** Normalised plot of the absorbance intensities of *apo*-MF2 (10 µM) at 377 nm in the absence (filled circles) or presence of AdcAI (5 µM; empty circles). Competition with Hst5 (10 µM; crosses) is shown for comparison. **(B) The tight site. (i)** Observed spectral changes upon titration of Zn (0 – 25 µM) into a mixture of *apo*-Q2 (7.5 µM) and AdcAI (10 µM). Downwards arrow indicates decreases in absorbance intensity. **(ii)** Normalised plot of the absorbance intensities of *apo*-Q2 (7.5 µM) at 262 nm upon addition of Zn (0 – 25 µM) in the absence (filled circles) or presence (empty circles) of AdcAI (10 µM).

Under the same experimental conditions, Hst5 did not compete with Mf2 for Zn (Figure 9A), consistent with the weak affinity of this peptide for Zn. These *relative* affinities, determined under the *same* conditions, support the hypothesis that Hst5 does not compete with AdcAI for binding Zn, and provides a molecular explanation for why this peptide does not limit the availability of extracellular nutrient Zn to wild-type GAS.

Hst5 did not affect growth of GAS even when AdcAI was deleted by mutagenesis (*cf.* Figure 5D), indicating that this peptide does not compete with other high-affinity Zn uptake proteins such as AdcAII (*cf.* Figure 3). AdcAII was expressed here for metal competition assays. However, consistent with a previous report[49], it was co-purified with 1 molar equiv. of bound Zn, which could not be removed without denaturing the protein. Nevertheless, the reported affinity of the *S. pneumoniae* homologue (log K_{Zn} = 7.7, 67% identity, 81% similarity), determined *via* competition with Mf2[50], is consistent with our proposal that Hst5 does not compete effectively with AdcAII for binding Zn.

Taken together with the lack of an observable Zn starvation phenotype (*cf.* Figure 5A-D), we conclude that, contrary to our original hypothesis, Hst5 does not participate in nutritional immunity against GAS by limiting Zn availability. Here, the human protein calprotectin provides a useful contrast. Calprotectin binds two Zn ions with affinities (log K_{Zn} >11 and >9.6)[51] that are comparable to those of AdcAI and tighter than that of AdcAII. Indeed, adding calprotectin induces a robust Zn starvation response in streptococci[52, 53], consistent with its established role in nutritional immunity.

Its low affinity to Zn also explains why Hst5 only weakly influences availability of *excess* Zn to GAS *in vitro*. Our growth medium[20] contains phosphate (~6 mM) and amino acids (~6 mM total), which would outcompete Hst5 (50 µM) for binding Zn[46]. As these media components become depleted during bacterial growth, they would become less competitive, allowing Hst5 to bind Zn and affect extracellular Zn speciation more strongly, particularly when Zn concentrations are high. Such shifts in Zn speciation may explain why the protective effect of Hst5 on the Δ*czcD* mutant during conditions of Zn stress became apparent only at the later stages of growth (*cf.* Figures 5F-G). At this point, increased binding of Zn to Hst5 may suppress *non-specific* Zn import into the GAS cytoplasm, for instance by outcompeting promiscuous divalent metal transporters or by suppressing direct Zn diffusion across the lipid bilayer. *In vivo*, saliva contains ~10 mM phosphate[54, 55] and proteinaceous components that may also buffer Zn[56]. Unlike *in vitro* growth media, saliva and its components are continuously refreshed. Therefore, Hst5 is unlikely to strongly influence Zn speciation and availability in saliva.

Molecular basis for the observed action of Hst5 as a strong Cu buffer.

Hst5 binds one Cu(II) atom with log K_{Cu} = 11.1, as determined previously by competition with NTA[18]. Since both Hst5 and NTA have weak optical signals (Figure S8), this Cu(II) affinity was re-examined here using PAR as an intensely coloured mediator[57] between NTA and Hst5. In the control titration, adding Cu(II) to *apo*-PAR decreased the *apo*-PAR absorbance at 400 nm and concomitantly increased the Cu(II)-PAR absorbance at 512 nm (Figure 10A). As anticipated[58], this titration produced an end point at 1:1 Cu(II):PAR (Figure S9A). Adding Cu(II) into *apo*-PAR in the presence of 20 molar equiv. each of NTA or Hst5 led to an effective competition between PAR and each of the competing ligands (Figure 10B-C). The competition curves yielded a log K_{Cu} = 12.1 (±0.1) for Hst5 (Figure 10C, Figure S9B-C), ~10-fold tighter than estimates from direct competition with NTA[18]. As previously acknowledged, the weak solution absorbances of Cu^{II}-NTA and Cu^{II}-Hst5 complexes did not saturate even in the presence of excess Cu (Figure S8B), indicating potential Cu-buffer interactions that were not accounted in the calculations, which may explain the slight underestimate[18, 59].

Consistent with an earlier report[18], deletion of either *bis*-His motif did not affect the competition between Hst5 and PAR (Figure 10C), confirming that these residues do not participate in binding Cu(II). By contrast, deletion of His3 abolished the competition with PAR (Figure 10C), confirming the ATCUN motif as Cu(II) binding ligands. More precise affinities for these variants were obtained *via* competition with the fluorometric Cu(II) chelator DP2[60]. By monitoring quenching of *apo*-DP2 fluorescence at 550 nm, the competition curves yielded log K_{Cu} values of 9.3 (±1.0) and 9.4 (±0.8) for the ΔH3 and ΔH3,H7 variants, respectively (Figure S9D). These values indicate that loss of the ATCUN His weakened the affinity of Hst5 by ~100-fold.

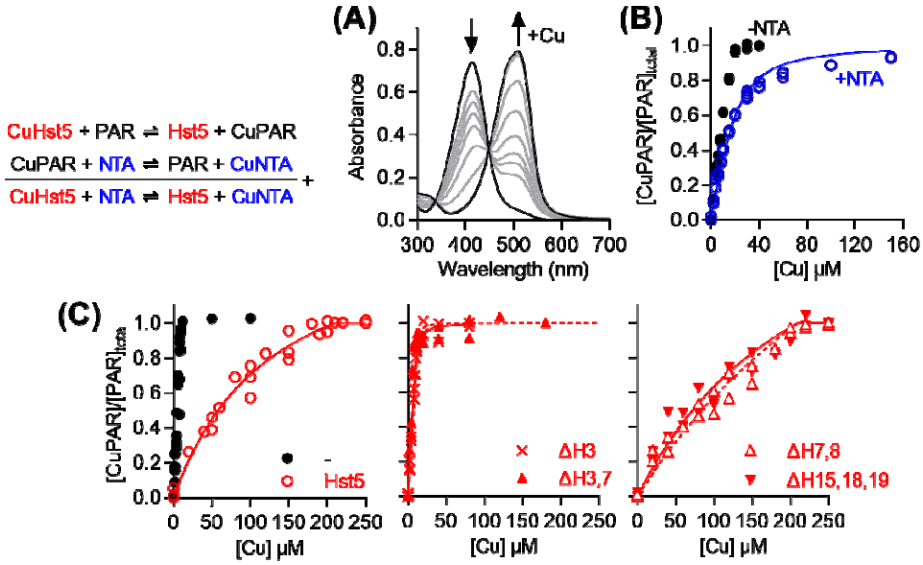

Figure 10. Cu(II) affinity of Hst5. (A) Spectral changes upon titration of Cu(II) (0 – 160 μM) into *apo*-PAR (20 μM). Upwards and downwards arrows indicate increases and decreases in absorbance intensity, respectively. **(B)** Normalised plot of the absorbance intensities of CuPAR at 512 nm upon titration of Cu into *apo*-PAR (20 μM) in the absence or presence of NTA (400 μM). **(C)** Normalised plot of the absorbance intensities of CuPAR at 512 nm upon titration of Cu into *apo*-PAR (10 μM) in the absence or presence of Hst5 peptides (200 μM).

The high affinity of Hst5 to Cu(II) explains why this peptide strongly suppresses Cu availability to GAS *in vitro* (*cf.* Figure 7). We hypothesise that Hst5 outcompetes transporters that catalyse *non-specific* Cu(II) uptake into GAS. This model will need to be tested by directly competing Hst5 and these transporters *in vitro*, but the latter are yet to be identified and are likely to be diverse. Nevertheless, the results here confirm that, contrary to our original hypothesis, Hst5 does not participate in nutritional immunity against GAS by increasing Cu availability and promoting Cu toxicity.

Does Hst5 contribute to nutritional immunity by suppressing *nutrient* Cu availability and causing Cu starvation? The GAS genome does not encode Cu-dependent proteins or enzymes, and so this bacterium is not thought to use or uptake nutrient Cu. Therefore, this proposal will need to be tested using other microbes that do need nutrient Cu. Nevertheless, parallels can be drawn with calprotectin, which binds two Cu(II) ions with affinities (*log* K_{Cu} = -11.4 and 12.7)[61] that are comparable to that of Hst5. Treatment with calprotectin induces a Cu starvation response in *C. albicans*[61]. Yet, Hst5 activity against this fungus appears linked to Cu excess and not Cu starvation[18]. Thus, the potential role of Hst5 in limiting nutrient Cu awaits further investigation.

DISCUSSION

GAS is a bacterial pathogen that causes over 600 million cases of pharyngitis each year[62], although asymptomatic carriage in the oropharynx is common, especially among children[63]. This host niche is rich in saliva, and the interactions between GAS and the components of this host fluid

are key for colonisation, infection, and subsequent transmission of this bacterium.[64-66] For example, exposure to saliva promotes aggregation of GAS and may thus block adherence to mucosal epithelia.[67] However, this bacterium produces surface adhesins that aid in binding to host mucosal surfaces.[68] Saliva also contains polysaccharides and glycoproteins that may serve as sources of nutrients. Accordingly, GAS genes involved in carbohydrate utilisation are highly expressed upon exposure to saliva[69] and mutant strains lacking these genes show decreased fitness in saliva[70].

Given the widely reported antimicrobial activity of Hst5 *in vitro*, salivary histatins are thought to act as antimicrobial peptides. Yet, our work shows that Hst5 does not kill or inhibit growth of GAS, particularly under saliva-relevant conditions. Given the metal-binding properties of Hst5, salivary histatins have been proposed to contribute to nutritional immunity, but our data establish that Hst5 does not starve GAS of nutrient Zn, nor does it enhance Cu toxicity to this bacterium. Our findings are consistent with the results from a genome-wide screen of a GAS mutant library, which did not identify Zn uptake or Cu efflux genes as essential for growth in saliva[70].

Thus far, discussions of the physiological role of histatins have focused on the likely antagonistic relationship between these peptides and opportunistic oral pathogens *in vivo*. By comparison, little is known about the potentially harmonious relationship between histatins and microbes that normally colonise healthy oral and oropharyngeal tissues. We showed here that Hst5 does not kill oral streptococci, which represent the most abundant taxon in a healthy oral cavity[71-74] and oropharynx[75]. This lack of an anti-streptococcal effect contrasts with the potent antibacterial effects of Hst5 against several ESKAPE pathogens[12], although the latter are worth revisiting to ensure that they are not associated with artificial experimental conditions that do not mimic the saliva.

It is worth noting that, while total levels of intact, full-length Hst5 and other major histatins in fresh salivary gland secretions are relatively high (up to 50 μM)[10], steady-state levels in whole saliva are low[10], a consequence of rapid peptide degradation by unidentified salivary proteases and proteases from resident oral microbes[76, 77]. Nearly fifty distinct histatin-derived peptide fragments have been identified[33, 78]. These fragments are generally associated with reduced antimicrobial activities[9, 33], raising the question whether an antimicrobial role is the major physiological role for Hst5 (or indeed the other histatins).

Intriguingly, proteolytic cleavage of histatins in saliva typically leads to retention of the original Cu(II)-binding ATCUN motif (DSH-) and simultaneous generation of new ATCUN motifs as byproducts (RHH-, EKH-, KFH-, KRH-, KHH-, HSH-)[33]. These diverse new fragments likely continue to bind Cu(II)[79], thus raising the intriguing possibility that Cu binding is the key role for Hst5 and the other histatins. The results described here are certainly consistent with this proposal.

We speculate that histatins contribute to oral and oropharyngeal health by buffering Cu availability. Steady-state levels of Cu in healthy saliva are sub-stoichiometric relative to histatins[41-43], but additional Cu enters the oral cavity through food (*e.g.* liver, shellfish, dark chocolate) or food supplements (*e.g.* multivitamins). In addition, Cu levels in saliva can also rise during periodontal diseases[80-82]. By buffering Cu, histatins may protect resident oral microbes from the potential toxic effects of a sudden or sustained exposure to *excess* Cu.

Streptococci do not need Cu as a nutrient, and so these bacteria likely benefit from the action

of histatins as Cu-buffering agents. This idea is not inconsistent with the relative dominance of *Streptococcus* species in the human oral cavity and oropharynx. However, other resident oral microbes, such as commensal *Neisseria* species and even *C. albicans*, need nutrient Cu for respiration and energy production. Do histatins buffer *nutrient* Cu availability to these microbes? The oral cavity and oropharynx are also major entry points for foreign pathogens that can cause oral, gut, and respiratory infections, many of which also need Cu as a nutrient. How is Cu availability managed, such that toxicity is limited to resident microbes but enhanced to foreign pathogenic microbes, and that nutrient supply is maintained to resident microbes but suppressed to pathogenic ones? Are there species-specific differences? What is the molecular basis of such differences? These studies are currently ongoing in our laboratory.

METHODS

Data presentation. Except for growth curves, individual data points from independent experiments are plotted, with shaded columns representing the means and error bars representing standard deviations. Growth curves show the means of independent experiments, with shaded regions representing standard deviations. The number of independent experiments is stated clearly in figure legends. Statistical analyses have been performed on all numerical data, but notations of statistical significance are displayed on plots only if they aid in rapid, visual interpretation. Otherwise, *P* values for key comparisons are stated in the figure legends. Unless otherwise stated, statistical tests used two-way analysis of variance using the statistical package in GraphPad Prism 8.0. All analyses were corrected for multiple comparisons.

Reagents. All reagents were of analytical grade from Merck or Melford Chemicals. Sulfate and chloride salts of metals were used interchangeably. All reagents were prepared in deionised water. Concentrations of fluorometric and colourimetric metal indicators (Zincon, PAR, Magfura-2, Quin-2, BCS, DP-2) were standardised using a commercial standard solution of copper chloride. Concentrations of optically silent chelators (NTA) were standardised by competition with a standardised solution of Zn-Zincon.

Synthesis and handling of Hst5 peptides. Initial preliminary work used peptides that were synthesised in-house as the TFA salt. Work described in this publication used peptides that were synthesised commercially as the acetate salt and purified to >95% (GenScript). Hst5 preparations were confirmed to be metal-free by ICP MS. Concentrations of stock peptide solutions were determined using solution absorbances at 280 nm in Mops buffer (50 mM, pH 7.4; ε_{280} = 2667 cm^{-1}).

Strains and culture conditions. All bacterial strains (Dataset S1b) were propagated from frozen glycerol stocks onto solid THY (Todd Hewitt + 0.2% yeast extract) medium without any antibiotics. Liquid cultures were prepared in THY or CDM-glucose[20]. All solid and liquid growth media contained catalase (50 μg/ml).

Survival assays. Fresh colonies from an overnight THY agar were resuspended to 10^6-10^7 CFU/mL in either potassium phosphate buffer (10 mM, pH 7.4), Mops buffer (10 mM, pH 7.4), or artificial salivary salts (pH 7.2; Dataset S1a). The cultures were incubated at 37 ^oC with or without Hst5 and/or metals as required. At *t* = 0, 1, and 3 h, cultures were sampled and serially diluted in

CDM-glucose. Exactly 10 µL of each serial dilution was spotted onto fresh THY agar. Colonies were enumerated after overnight incubation at 37 ^{o}C.

Growth assays. Colonies from an overnight THY agar were resuspended in CDM-glucose to an OD_{600} = 0.01. Growth was assessed at 37 °C in flat-bottomed 96-well plates (200 µL per well) using an automated microplate shaker and reader. Each plate was sealed with a gas permeable, optically clear membrane (Diversified Biotech). OD_{600} values were measured every 20 min for 10 h. The plates were shaken immediately before each reading (200 rpm, 1 min, double orbital mode). OD_{600} values were not corrected for path length (*ca*. 0.58 cm for a 200-µl culture).

RNA extraction. Colonies from an overnight THY agar were resuspended in CDM-glucose to an OD_{600} = 0.01 and incubated in 24-well plates (1.6 mL per well) without shaking at 37 ^{o}C. Each plate was sealed with a gas permeable, optically clear membrane (Diversified Biotech). At *t* = 4 h, cultures were centrifuged (4,000 x *g*, 4°C, 5 min) and bacterial pellets were resuspended immediately in RNAPro Solution (0.5 mL; MP Biomedicals). Bacteria were lysed in Lysing Matrix B and total RNA was extracted following manufacturer's protocol (MP Biomedicals). Crude RNA extracts were treated with RNase-Free DNase I (New England Biolabs). Complete removal of gDNA was confirmed by PCR using gapA-check-F/R primers (Dataset S1c). gDNA-free RNA was purified using Monarch RNA Clean-up Kit (New England Biolabs) and visualised on an agarose gel.

qRT-PCR analyses. cDNA was generated from RNA (1.6 µg) using SuperScript® IV First-Strand Synthesis System (Invitrogen). Each qRT-PCR reaction (20 µL) contained cDNA (5 ng) as template and the appropriate primer pairs (0.4 µM; Dataset S1c). Samples were analysed in technical duplicates. Amplicons were detected with Luna® Universal qRT-PCR Master Mix (New England Biolabs) in a CFXConnect Real-Time PCR Instrument (Bio-Rad Laboratories). C_q values were calculated using LinRegPCR[83] after correcting for amplicon efficiency. C_q values of technical duplicates were typically within ± 0.25 of each other. *holB*, which encodes DNA polymerase III, was used as reference gene. Its transcription levels remained constant in all of the experimental conditions tested here.

Intracellular metal content. Colonies from an overnight THY agar were resuspended in CDM-glucose to an OD_{600} = 0.02 and incubated at 37 ^{o}C with or without Hst5 and/or metals as required. At *t* = 4 h, an aliquot was collected for the measurement of plating efficiency (colony counts). The remaining cultures were harvested (5,000 g, 4 °C, 10 min), and washed once with ice-cold wash buffer (1 M *D*-sorbitol, 50 mM Tris-HCl, 10 mM $MgCl_2$, 1 mM EDTA, pH 7.4) and twice with ice-cold PBS. The final pellets were dissolved in concentrated nitric acid (100 µL), heated (85 °C, 1.5 h), and diluted to 3.5 mL with 2 % nitric acid. Total metal levels were determined by ICP MS. The results were normalised to colony counts.

Elution of Zn-Hst5 on a desalting column. *Apo*-Hst5 (100 µM) was incubated with 1.5 molar equiv. of Zn for 15 min at the bench and loaded onto a polyacrylamide desalting column (1.8 kDa molecular weight cutoff, Thermo Scientific). Peptide content in each fraction was verified using QuantiPro BCA Assay Kit (Merck). Zn content was determined using PAR against a standard curve.

Equilibrium competition reactions. For each competition (eq 1 below), a master stock was prepared to contain both competing ligands (L1 and L2) in Mops buffer (50 mM, pH 7.4). Serial

dilutions of the metal (M) were prepared separately in deionised water. Exactly 135 µL of the master stock was dispensed into an Eppendorf UVette and 15 µL of the appropriate metal stock was added. Solution absorbances were used to calculate concentrations of *apo*- and metalated forms of the relevant ligand. These concentrations were plotted against metal concentrations and fitted in DynaFit[84] using binding models as described in the text. The known association or dissociation constants for all competitor ligands are listed in Dataset S1d:

$M\text{-}L1_n + m\ L2$ ßà $n\ L1 + M\text{-}L2_m$ (eq. 1)

Overexpression and purification of AdcAI and AdcAII. Nucleic acid sequences encoding the soluble domains of AdcAI (from Thr21) and AdcAII (from Thr31) from M1GAS strain 5448 were subcloned into vector pSAT1-LIC using primers listed in Dataset S1c. This vector generates N-terminal His6-SUMO fusions with the target ORF. The resulting plasmids were propagated in *E. coli* Dh5α, confirmed by Sanger sequencing, and transformed into *E. coli* BL21 Rosetta 2(DE3).

To express the proteins, transformants were plated onto LB agar. Fresh colonies were used to inoculate LB (1 L in 2 L baffled flasks) to an OD_{600} of 0.01. The culture media contained ampicillin (100 µg/mL) and chloramphenicol (33 µg/mL) as required. Cultures were shaken (200 rpm, 37 °C) until an OD_{600} of 0.6–0.8 was reached, and expression was induced by adding IPTG (0.1 mM). After shaking for a further 16 h at 20 ^{o}C, the cultures were centrifuged (4000 × *g*, 4 °C) and the pellets were resuspended in buffer A500 (20 mM Tris–HCl, pH 7.9, 500 mM NaCl, 5 mM imidazole, 10% glycerol).

To purify proteins, bacteria were lysed by sonication (40 kpsi), centrifuged (20,000 × *g*, 4°C), and filtered through a 0.46 µm PES membrane filtration unit. Clarified lysates were loaded onto a HisTrap HP column (Cytiva). The column was washed with 10 column volumes (CV) of buffer A500 followed by 10 CV of buffer A100 (20 mM Tris–HCl, pH 7.9, 100 mM NaCl, 10% w/v glycerol) containing imidazole (5 mM). Both AdcAI and AdcAII were bound to the column and subsequently eluted with 3 CV of buffer A100 containing 250 mM imidazole followed by 5 CV of 500 mM imidazole. Protein-containing fractions were loaded onto a Q HP column (Cytiva). The column was washed with 5 CV of buffer A100 and bound proteins were eluted using a step gradient of 0, 10, 15, and 20% buffer C1000 (20 mM Tris–HCl, pH 7.9, 1000 mM NaCl, 10% w/v glycerol). Eluted proteins were incubated overnight at 4 °C with hSENP2 SUMO protease to cleave the His6-SUMO tag from the target protein. Samples were passed through a second Q HP column and the flowthrough fractions containing untagged target protein were collected.

AUTHOR CONTRIBUTIONS

KD conceived the project with input from NJ, SC. JH, KD, LS, NJ designed the experiments. IH, JH, SF measured the affinities of peptides to Zn and Cu. JH expressed AdcA proteins and measured their affinities to Zn. LS examined the effects of peptides on bacterial survival. IH, JH, KD, LS examined the effects of peptides on bacterial growth. JB, KD measured gene expression by qRT-PCR. KD, LS measured metal levels by ICP MS. NJ provided oral streptococci strains. IH, SC, YS synthesised peptides for preliminary studies. JH, KD, LS prepared figures and drafted the manuscript.

ACKNOWLEDGEMENT

This research was funded by the Wellcome Trust (grant number 214930/Z/18/Z). For the purpose of open access, the author has applied a CC BY public copyright licence to any Author Accepted Manuscript version arising from this submission. This project was also supported by a Flexible Funding Award from the Durham Biophysical Sciences Institute. SF and JB were supported by studentships from the BBSRC Newcastle-Liverpool-Durham Doctoral Training Partnership.

T Blower (Department of Biosciences, Durham University) provided constructs and reagents for the expression AdcAI and AdcAII. The Δ*adcAI* and Δ*czcD* mutant strains of GAS were kind gifts from C Ong, A McEwan, and M Walker (School of Chemistry and Molecular Biosciences, University of Queensland). Quin2 was generously donated by T Young (Department of Biosciences, Durham Univeristy). We thank R Borthwick (Department of Physics, Durham University), P Chivers (Department of Biosciences, Durham University), Y Ahmed and J Quinn (Newcastle University Biosciences Institute) for helpful discussions throughout the project.

REFERENCES

1. Hood, M.I. and E.P. Skaar, *Nutritional immunity: transition metals at the pathogen-host interface.* Nat Rev Microbiol, 2012. **10**(8): p. 525-37.
2. Zhang, L.J. and R.L. Gallo, *Antimicrobial peptides.* Curr Biol, 2016. **26**(1): p. R14-9.
3. Kim, S.Y., et al., *Copper regulates the interactions of antimicrobial piscidin peptides from fish mast cells with formyl peptide receptors and heparin.* J Biol Chem, 2018. **293**(40): p. 15381-15396.
4. Silva, F.D., et al., *Structure and mode of action of microplusin, a copper II-chelating antimicrobial peptide from the cattle tick Rhipicephalus (Boophilus) microplus.* J Biol Chem, 2009. **284**(50): p. 34735-46.
5. Silva, F.D., et al., *Effects of microplusin, a copper-chelating antimicrobial peptide, against Cryptococcus neoformans.* FEMS Microbiol Lett, 2011. **324**(1): p. 64-72.
6. Troxler, R.F., et al., *Structural relationship between human salivary histatins.* J Dent Res, 1990. **69**(1): p. 2-6.
7. Sabatini, L.M. and E.A. Azen, *Histatins, a family of salivary histidine-rich proteins, are encoded by at least two loci (HIS1 and HIS2).* Biochem Biophys Res Commun, 1989. **160**(2): p. 495-502.
8. Azen, E.A., W. Leutenegger, and E.H. Peters, *Evolutionary and dietary aspects of salivary basic (Pb) and post Pb (PPb) proteins in anthropod primates.* Nature, 1978. **273**(5665): p. 775-8.
9. Helmerhorst, E.J., et al., *Oral fluid proteolytic effects on histatin 5 structure and function.* Arch Oral Biol, 2006. **51**(12): p. 1061-70.
10. Campese, M., et al., *Concentration and fate of histatins and acidic proline-rich proteins in the oral environment.* Arch Oral Biol, 2009. **54**(4): p. 345-53.
11. Puri, S. and M. Edgerton, *How does it kill?: understanding the candidacidal mechanism of salivary histatin 5.* Eukaryot Cell, 2014. **13**(8): p. 958-64.

12. Du, H., et al., *Human Salivary Protein Histatin 5 Has Potent Bactericidal Activity against ESKAPE Pathogens.* Front Cell Infect Microbiol, 2017. **7**: p. 41.
13. Mochon, A.B. and H. Liu, *The antimicrobial peptide histatin-5 causes a spatially restricted disruption on the Candida albicans surface, allowing rapid entry of the peptide into the cytoplasm.* PLoS Pathog, 2008. **4**(10): p. e1000190.
14. Helmerhorst, E.J., et al., *The cellular target of histatin 5 on Candida albicans is the energized mitochondrion.* The Journal of Biological Chemistry, 1999. **274**(March 12).
15. Helmerhorst, E.J., et al., *Synthetic histatin analogues with broad-spectrum antimicrobial activity.* Biochem J, 1997. **326**: p. 39–45.
16. Norris, H.L., et al., *Zinc Binding by Histatin 5 Promotes Fungicidal Membrane Disruption in C. albicans and C. glabrata.* J Fungi (Basel), 2020. **6**(3).
17. Puri, S., et al., *Iron binding modulates candidacidal properties of salivary histatin 5.* J Dent Res, 2015. **94**(1): p. 201-8.
18. Conklin, S.E., et al., *Specific Histidine Residues Confer Histatin Peptides with Copper-Dependent Activity against Candida albicans.* Biochemistry, 2017. **56**(32): p. 4244-4255.
19. Turner, A.G., et al., *Transition Metal Homeostasis in Streptococcus pyogenes and Streptococcus pneumoniae.* Adv Microb Physiol, 2017. **70**: p. 123-191.
20. Stewart, L.J., et al., *Role of Glutathione in Buffering Excess Intracellular Copper in Streptococcus pyogenes.* mBio, 2020. **11**(6): p. e02804-20.
21. Li, X.S., et al., *Candida albicans cell wall ssa proteins bind and facilitate import of salivary histatin 5 required for toxicity.* J Biol Chem, 2006. **281**(32): p. 22453-63.
22. Jang, W.S., et al., *The P-113 fragment of histatin 5 requires a specific peptide sequence for intracellular translocation in Candida albicans, which is independent of cell wall binding.* Antimicrob Agents Chemother, 2008. **52**(2): p. 497-504.
23. Yu, H.Y., et al., *Easy strategy to increase salt resistance of antimicrobial peptides.* Antimicrob Agents Chemother, 2011. **55**(10): p. 4918-21.
24. Han, J., et al., *Antifungal Activity and Action Mechanism of Histatin 5-Halocidin Hybrid Peptides against Candida ssp.* PLoS One, 2016. **11**(2): p. e0150196.
25. Helmerhorst, E.J., et al., *Dialysis unmasks the fungicidal properties of glandular salivary secretions.* Infect Immun, 2004. **72**(5): p. 2703-9.
26. Meurer, M., et al., *Antimicrobial Susceptibility Testing of Antimicrobial Peptides Requires New and Standardized Testing Structures.* ACS Infect Dis, 2021. **7**(8): p. 2205-2208.
27. Fernandez-Presas, A.M., et al., *Ultrastructural damage in Streptococcus mutans incubated with saliva and histatin 5.* Arch Oral Biol, 2018. **87**: p. 226-234.
28. MacKay, B.J., et al., *Growth-inhibitory and bactericidal effects of human parotid salivary histidine-rich polypeptides on Streptococcus mutans.* Infect Immun, 1984. **44**: p. 695-701.
29. Tian, X.L., et al., *The BceABRS four-component system that is essential for cell envelope stress response is involved in sensing and response to host defence peptides and is required for the biofilm formation and fitness of Streptococcus mutans.* J Med Microbiol, 2018. **67**(6): p. 874-883.

30. Andrian, E., et al., *Role of surface proteins SspA and SspB of Streptococcus gordonii in innate immunity.* Microbiology (Reading), 2012. **158**(Pt 8): p. 2099-2106.
31. Krzyściak, W., et al., *Effect of histatin-5 and lysozyme on the ability of Streptococcus mutans to form biofilms in in vitro conditions.* Postepy Hig Med Dosw (online), 2015. **69**: p. 1056-1066.
32. Helmerhorst, E.J., et al., *The Effects of Histatin-derived Basic Antimicrobial Peptides on Oral Biofilms.* J Dent Res, 1999. **78**(6): p. 1245-1250.
33. Hardt, M., et al., *Toward Defining the Human Parotid Gland Salivary Proteome and Peptidome.* Biochemistry, 2005. **44**(8): p. 2885-2899.
34. Greger, J.L. and V.S. Sickles, *Saliva zinc levels: potential indicators of zinc status.* The American Journal of Clinical Nutrition, 1979. **32**: p. 1859-1866.
35. Sanson, M., et al., *Adhesin competence repressor (AdcR) from Streptococcus pyogenes controls adaptive responses to zinc limitation and contributes to virulence.* Nucleic Acids Res, 2015. **43**(1): p. 418-32.
36. Ong, C.L., et al., *An antimicrobial role for zinc in innate immune defense against group A streptococcus.* J Infect Dis, 2014. **209**(10): p. 1500-8.
37. Tedde, V., R. Rosini, and C.L. Galeotti, *Zn2+ Uptake in Streptococcus pyogenes: Characterization of adcA and lmb Null Mutants.* PLoS One, 2016. **11**(3): p. e0152835.
38. Ong, C.L., et al., *New Insights into the Role of Zinc Acquisition and Zinc Tolerance in Group A Streptococcal Infection.* Infect Immun, 2018. **86**(6): p. e00048-18.
39. Grogan, J., et al., *Zinc and copper bind to unique sites of histatin 5.* FEBS J, 2001. **491**: p. 76-80.
40. Melino, S., et al., *Zn(2+) ions Selectively Induce Antimicrobial Salivary Peptide Histatin-5 To Fuse Negatively Charged Vesicles. Identification and Characterization of a Zinc-Binding Motif Present in the Functional Domain.* Biochemistry, 1999. **38**: p. 9626-9633.
41. Shetty, S.R., et al., *Status of trace elements in saliva of oral precancer and oral cancer patients.* J Cancer Res Ther, 2015. **11**(1): p. 146-9.
42. Duggal, M.S., H.S. Chawla, and M.E.J. Curzon, *A study of the relationship between trace elements in saliva and dental caries in children.* Archives of Oral Biology, 1991. **36**(12): p. 881-884.
43. Inonu, E., et al., *The Association Between Some Macro and Trace Elements in Saliva and Periodontal Status.* Biol Trace Elem Res, 2020. **197**(1): p. 35-42.
44. Young, C.A., et al., *Copper Tolerance and Characterization of a Copper-Responsive Operon, copYAZ, in an M1T1 Clinical Strain of Streptococcus pyogenes.* J Bacteriol, 2015. **197**(15): p. 2580-92.
45. Gusman, H., et al., *Is salivary histatin 5 a metallopeptide?* Biochimica et Biophysica Acta, 2001. **1545**: p. 86-95.
46. Krezel, A. and W. Maret, *The biological inorganic chemistry of zinc ions.* Arch Biochem Biophys, 2016. **611**: p. 3-19.

47. Cao, K., et al., *Two zinc-binding domains in the transporter AdcA from Streptococcus pyogenes facilitate high-affinity binding and fast transport of zinc.* J Biol Chem, 2018. **293**(16): p. 6075-6089.
48. Young, T.R. and Z. Xiao, *Principles and practice of determining metal-protein affinities.* Biochem J, 2021. **478**(5): p. 1085-1116.
49. Linke, C., et al., *The laminin-binding protein Lbp from Streptococcus pyogenes is a zinc receptor.* J Bacteriol, 2009. **191**(18): p. 5814-23.
50. Zupan, M.L., et al., *Conformation of the Solute-Binding Protein AdcAII Influences Zinc Uptake in Streptococcus pneumoniae.* Front Cell Infect Microbiol, 2021. **11**: p. 729981.
51. Brophy, M.B., J.A. Hayden, and E.M. Nolan, *Calcium ion gradients modulate the zinc affinity and antibacterial activity of human calprotectin.* J Am Chem Soc, 2012. **134**(43): p. 18089-100.
52. Makthal, N., et al., *A Critical Role of Zinc Importer AdcABC in Group A Streptococcus-Host Interactions During Infection and Its Implications for Vaccine Development.* EBioMedicine, 2017. **21**: p. 131-141.
53. Burcham, L.R., et al., *Identification of Zinc-Dependent Mechanisms Used by Group B Streptococcus To Overcome Calprotectin-Mediated Stress.* mBio, 2020. **11**(6).
54. Hartman, M.L., et al., *Can salivary phosphate levels be an early biomarker to monitor the evolvement of obesity?* Contrib Nephrol, 2013. **180**: p. 138-48.
55. Savica, V., et al., *Phosphate salivary secretion in hemodialysis patients: implications for the treatment of hyperphosphatemia.* Nephron Physiol, 2007. **105**(3): p. p52-5.
56. Lynge Pedersen, A.M. and D. Belstrom, *The role of natural salivary defences in maintaining a healthy oral microbiota.* J Dent, 2019. **80 Suppl 1**: p. S3-S12.
57. Zimmermann, M., et al., *Metal specificities of Arabidopsis zinc and copper transport proteins match the relative, but not the absolute, affinities of their N-terminal domains.* Chem Commun (Camb), 2009(42): p. 6364-6.
58. Doyle, C.M., et al., *Spectrophotometric method for simultaneous measurement of zinc and copper in metalloproteins using 4-(2-pyridylazo)resorcinol.* Anal Biochem, 2019. **579**: p. 44-56.
59. Rozga, M., et al., *Human serum albumin coordinates Cu(II) at its N-terminal binding site with 1 pM affinity.* J Biol Inorg Chem, 2007. **12**(6): p. 913-8.
60. Young, T.R., et al., *A set of robust fluorescent peptide probes for quantification of Cu(ii) binding affinities in the micromolar to femtomolar range.* Metallomics, 2015. **7**(3): p. 567-78.
61. Besold, A.N., et al., *Role of Calprotectin in Withholding Zinc and Copper from Candida albicans.* Infect Immun, 2018. **86**(2).
62. Carapetis, J.R., et al., *The global burden of group A streptococcal diseases.* Lancet Infect Dis, 2005. **5**(11): p. 685-94.
63. Shaikh, N., E. Leonard, and J.M. Martin, *Prevalence of streptococcal pharyngitis and streptococcal carriage in children: a meta-analysis.* Pediatrics, 2010. **126**(3): p. e557-64.

64. Hamburger, M. and O.H. Robertson, *Expulsion of group a hemolytic streptococci in droplets and droplet nuclei by sneezing, coughing and talking.* The American Journal of Medicine, 1948. **4**(5): p. 690-701.
65. Hamburger Jr, M., *Studies on the transmission of hemolytic streptococcus infections: II. Beta hemolytic streptococci in the saliva of persons with positive throat cultures.* The Journal of Infectious Diseases, 1944: p. 71-78.
66. Courtney, H.S. and D.L. Hasty, *Aggregation of group A streptococci by human saliva and effect of saliva on streptococcal adherence to host cells.* Infect Immun, 1991. **59**(5): p. 1661-6.
67. Courtney, H. and D. Hasty, *Aggregation of group A streptococci by human saliva and effect of saliva on streptococcal adherence to host cells.* Infection and immunity, 1991. **59**(5): p. 1661-1666.
68. Brouwer, S., et al., *Streptococcus pyogenes adhesion and colonization.* FEBS Letters, 2016. **590**(21): p. 3739-3757.
69. Shelburne, S.A., 3rd, et al., *Central role of a bacterial two-component gene regulatory system of previously unknown function in pathogen persistence in human saliva.* Proceedings of the National Academy of Sciences of the United States of America, 2005. **102**(44): p. 16037-16042.
70. Zhu, L., et al., *Novel Genes Required for the Fitness of Streptococcus pyogenes in Human Saliva.* mSphere, 2017. **2**(6): p. e00460-17.
71. Bik, E.M., et al., *Bacterial diversity in the oral cavity of 10 healthy individuals.* ISME J, 2010. **4**(8): p. 962-74.
72. Zaura, E., et al., *Defining the healthy "core microbiome" of oral microbial communities.* BMC Microbiol, 2009. **9**: p. 259.
73. Dewhirst, F.E., et al., *The human oral microbiome.* J Bacteriol, 2010. **192**(19): p. 5002-17.
74. Aas, J.A., et al., *Defining the normal bacterial flora of the oral cavity.* J Clin Microbiol, 2005. **43**(11): p. 5721-32.
75. Bach, L.L., et al., *A Longitudinal Study of the Human Oropharynx Microbiota Over Time Reveals a Common Core and Significant Variations With Self-Reported Disease.* Frontiers in Microbiology, 2021. **11**(3545).
76. Bochenska, O., et al., *The action of ten secreted aspartic proteases of pathogenic yeast Candida albicans on major human salivary antimicrobial peptide, histatin 5.* Acta Biochim Pol, 2016. **63**(3): p. 403-10.
77. Ikonomova, S.P., et al., *Effects of histatin 5 modifications on antifungal activity and kinetics of proteolysis.* Protein Sci, 2020. **29**(2): p. 480-493.
78. Vitorino, R., et al., *Towards defining the whole salivary peptidome.* PROTEOMICS - Clinical Applications, 2009. **3**(5): p. 528-540.
79. Gonzalez, P., et al., *N-Terminal Cu-Binding Motifs (Xxx-Zzz-His, Xxx-His) and Their Derivatives: Chemistry, Biology and Medicinal Applications.* Chemistry, 2018. **24**(32): p. 8029-8041.

80. Herman, M., et al., *Essential and Toxic Metals in Oral Fluid-a Potential Role in the Diagnosis of Periodontal Diseases.* Biol Trace Elem Res, 2016. **173**(2): p. 275-82.
81. Manea, A. and M. Nechifor, *Research on Plasma and Saliva Levels of Some Bivalent Cations in Patients with Chronic Periodontitis (Salivary Cations in Chronic Periodontitis)* Rev. Med. Chir. Soc. Med. Nat., Iaşi 2014. **118**(2): p. 439-449.
82. Romano, F., et al., *ICP-Mass-Spectrometry Ionic Profile of Whole Saliva in Patients with Untreated and Treated Periodontitis.* Biomedicines, 2020. **8**(9).
83. Ramakers, C., et al., *Assumption-free analysis of quantitative real-time polymerase chain reaction (PCR) data.* Neurosci Lett, 2003. **339**(1): p. 62-6.
84. Kuzmic, P., *DynaFit--a software package for enzymology.* Methods Enzymol, 2009. **467**: p. 247-280.